Plot-to-track correlation in A-SMGCS using the target images from a Surface Movement Radar

G. Golino
Radar & Technology Division
AMS, Italy
ggolino@amsjv.it

A. Farina
Chief Technical Office
AMS, Italy
afarina@amsjv.it

Abstract *The main topic of this paper is the formulation and performance evaluation of a novel plot-to-track correlation logic for the A-SMGCS (Advanced Surface Movement Guidance and Control System). The conventional plot-track logic exploits the kinematics information only. This logic might fail when more targets move in close proximity. Currently, high resolution radars - integrated in the A-SMGCS - are able to provide the electromagnetic image of the detected targets. Thus, the idea is to exploit also this target feature to improve the plot-track logic. The performance of the new algorithm is evaluated by Monte Carlo simulation using a realistic scenario corresponding to an airport where two targets move in close proximity on the airport surface.*

Keywords: Advanced Surface Movement Guidance and Control System (A-SMGCS), Surface Movement Radar (SMR), Imaging.

1 Introduction

The Advanced Surface Movement Guidance and Control System (A-SMGCS) is an integrated airport management system consisting of different functions (surveillance, control, guidance and routing) to support the safe, orderly and expeditious movement of aircraft and vehicles on aerodromes under all circumstances with respect to visibility conditions, traffic density and complexity of the aerodrome layout [1]. The main sensor of the A-SMGCS is the Surface Movement Radar (SMR), whose high resolution in range and azimuth provides an image of the target. The tracker of the A-SMGCS should manage the presence of numerous targets with very small spatial separation. The plot-to-track association algorithm of a conventional tracker is based on the distance between the predicted measurement and the measured plot. The closeness of the targets on the airport surface and the presence of heavy clutter can easily degrade performance causing lost, swapped or collapsed tracks. The target images from the SMR can be used, jointly to the information on distance, in the plot-to-track correlation algorithm to improve the probability of correct association. Because distance and electromagnetic image are not homogeneous characteristics, the correlation test must be decomposed in two separated tests, one using the distance information and the other exploiting the image information; these are successively fused by a combination logic. This two-step test (combined test) uses jointly both information to improve the correct plot-to-track association. In this paper the advantage of using an algorithm combining the information on distance between plot and track and data from a high resolution image of the target to help the correct association has been proven. A combined test is able to provide target enhanced discrimination capability with small dependency on target distance and it can be used to avoid tracking errors when two tracks are close to each other. We used in our analysis detection probability (P_d)=1 and zero false alarm density.

2 Integration of an image-based test in the plot-to-track correlation algorithm

In a multi target scenario, there can be tracking errors caused by the mixing of plots belonging to different targets. This event can happen when the correlation gates of two or more tracks overlap [2]. In this paper the analysis is limited to the case of two tracks (see Figure 1).

In low resolution radar the plot-to-track association is based only on the information on the distance between the predicted position of the target and the measured one [2]. On the other hand high resolution radar can also provide either the information on the target range profile (e.g. Radar Cross Section - RCS - along range) or target electromagnetic image (e.g. RCS along range and along azimuth). The target range profile or target image can be used jointly to the information on distance in the plot-to-track association problem to improve the probability of correct association. Because distance and electromagnetic range profile or image are not homogeneous characteristics, the correlation test must be decomposed in two separated tests, one using the distance information and the other exploiting the range profile or image information. these are successively fused by a combination logic (see Figure 2). In the figure the letters T and P represent respectively the track and the plot, while IMAGE_T and IMAGE_P represent respectively the image associated with the track T plot P. The image of the track is the image corresponding to the last plot correlated with the track. The output of the tests on distance and on

image can be either binary (0 or 1) or it can vary in the interval (0,1).

The plot-to-track association logic block diagram is shown in Figure 3 for the simplest case of two tracks and two plots. The inputs are two tracks T_1, T_2, with their relative images IMAGE_T_1 and IMAGE_T_2, and two plots P_1, P_2, qualified by the target position measurements, with their relative images IMAGE_P_1 and IMAGE_P_2; the outputs are all the combinations of plot-to-track associations. The association logic uses four combined tests as shown in Figure 3. The results of the combined tests are then processed by a suitable selection logic.

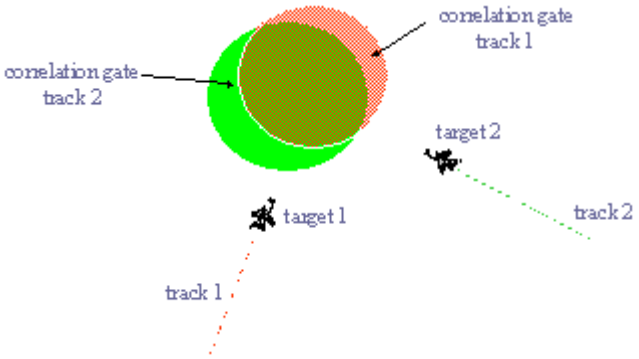

Figure 1. An example of overlapping of correlation gates.

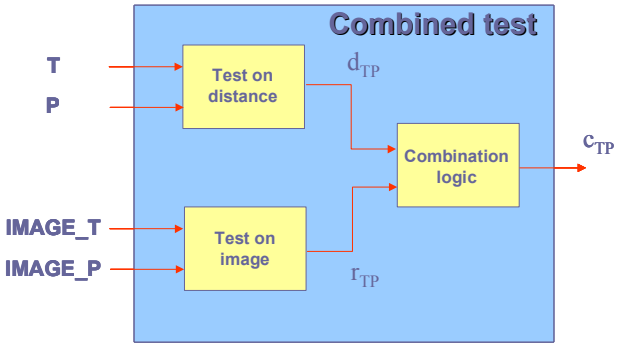

Figure 2. Block diagram of the test that combines the information on the distance and electromagnetic image of the target. Label T and P in figure: T: Track, P: Plot.

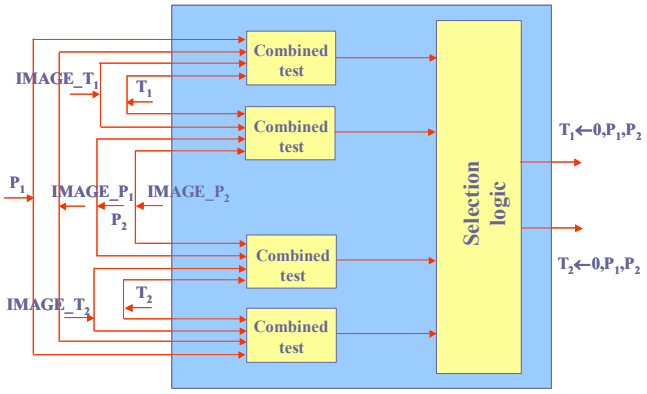

Figure 3. Block diagram of the plot-to-track association logic using kinematics data and the target images; the scheme is limited to the case of 2 tracks and 2 plots. The block "combined test" is the one in Figure 2.

3 Example of plot-to-track correlation algorithm using both distance and image

In this section an example of plot-to-track correlation algorithm using both distance and electromagnetic images is described. The simulation results reported in the following sections are obtained by using this algorithm.

The test on distance is based on the uncertainty ellipsoid of the considered track; it is defined as:

$$e_T \equiv \left\{ \left(\mathbf{z}(k) - \mathbf{H}\cdot\mathbf{s}(k)\right)^T \cdot \left(\mathbf{H}\cdot\mathbf{P}(k)\cdot\mathbf{H}^T + \mathbf{R}(k)\right)^{-1} \cdot \left(\mathbf{z}(k) - \mathbf{H}\cdot\mathbf{s}(k)\right) < h^2 \right\} \quad (1)$$

where:

- $\mathbf{z}(k)$ is the vector containing the target position measured by the radar and $\mathbf{R}(k)$ is its covariance matrix;
- $\mathbf{s}(k)$ is the vector containing the target state predicted by the tracking algorithm and $\mathbf{P}(k)$ is its covariance matrix;
- $\mathbf{H}$ is the matrix which relates the target state to the target position;
- h is a quantity related to the desired probability of finding the plot that should be associated to the track inside the uncertainty ellipsoid (in the simulations we set $h = 3$).

The test on distance has a binary output; it is one if the plot P is within the considered uncertainty ellipsoid, otherwise it is zero:

$$d_{TP} = \begin{cases} 1 & if \;\; P \in e_T \\ 0 & if \;\; P \notin e_T \end{cases} \quad (2)$$

The output of the test on image is the correlation coefficient of the two considered images:

$$r_{TP} = \frac{IMAGE\_T \otimes IMAGE\_P}{\sqrt{(IMAGE\_T \otimes IMAGE\_T)\cdot(IMAGE\_P \otimes IMAGE\_P)}} \quad (3)$$

where $\otimes$ denotes the correlation operator.

The combination logic of the combined test performs the multiplication of the outputs of the test on distance and the test on images:

$$c_{TP} = d_{TP} \cdot r_{TP} \quad (4)$$

Finally, the selection logic does not associate any plot if both the outputs of the combined tests are zero; otherwise it associates to the track the plot relative to the test with the higher output:

$$\begin{cases} T \leftarrow 0 & if \quad c_{TP_1} = c_{TP_2} = 0 \\ T \leftarrow P_1 & if \quad c_{TP_1} > c_{TP_2} \\ T \leftarrow P_2 & if \quad c_{TP_2} > c_{TP_1} \end{cases} \quad (5)$$

4 Scenario for testing the plot-to-track association algorithm

The following scenario has been considered: an aircraft (similar to a Boeing 747) lands on a runway and goes to the apron; while a car moves in the same direction along a taxiway close to the runway.

Figure 4 shows the trajectories of the aircraft and of the car. A section of a generic airport has been considered. The trajectories are sampled by an SMR with scan period equal to 1 s.

The two trajectories are very close for some seconds and the distance between the aircraft and the car reaches a minimum of about 50 metres (see Figure 5).

The standard deviations of the radar measurements have been set to 15 m in range and to 0.45° in azimuth for the plots coming from the airplane; it is 5 m in range and 0.15° in azimuth for the plots coming from the car. The standard deviation of the radar measurement concerning the airplane is assumed to be larger because of the stronger glint phenomenon due to the larger size of the airplane. The correlation gates of the two tracks are overlapped for the first thirty scans and this causes either swapping or collapsing of the tracks. Figure 6 and Figure 7 show an example of collapsing tracks obtained during a Monte Carlo simulation of the tracking algorithm [1]; Figure 8 shows instead an example of swapped tracks.

To calculate the electromagnetic images of the aircraft and of the car a simple "hot spots" model has been considered (see [3]); specifically on the geometrical structure of the target some hot spots have been located and set as source of the backscattered power (due to geometrical discontinuities). The electromagnetic images of the aircraft and of the car have been computed coherently summing the contributions of the single sources which can interfere either positively or negatively depending on the transmitted frequency and on the angle of view of the target.

Figure 9 shows a CAD model of the Boeing 747; 48 hot spots are highlighted on it. An RCS of 0.1 m^2 has been assigned to each hot spot. Figure 10 shows a CAD model of the car, a Volkswagen Beetle; 22 hot spots are selected and highlighted on it. An RCS of 0.02 m^2 has been assigned to each hot spot.

The considered transmitted frequency of the radar is 9 GHz, while the resolution has been fixed to 6 m in range and 0.5° in azimuth. These are typical values of an SMR. The SNR with respect to an RCS target of 1 m^2 has been fixed to 40 dB along the trajectory.

Figure 11 shows some example of the aircraft electromagnetic images along the trajectory of Figure 4. The x-coordinate represents the across-range dimension, while y-coordinate represents the along range dimension. It can be noted that the image of the aircraft changes considerably during the trajectory due to the changing of angle of view. However the images concerning consecutive scans are strongly correlated because of the very small variation of the angle of view; this feature is exploited by the plot-to-track association logic using images to improve the tracking algorithm performance.

Figure 12 shows some example of the car electromagnetic images along the trajectory of Figure 4. It can be noted that, because of the limited dimensions and the limited changing of the angle of view, the electromagnetic image does not vary sensibly along the trajectory.

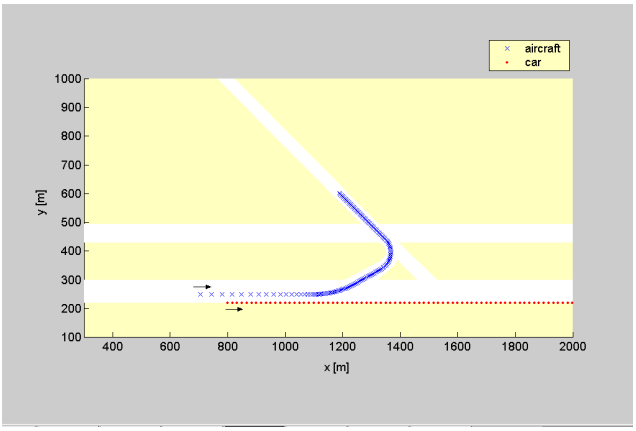

Figure 4. Samples of the trajectory of an aircraft (blue crosses) and a car (red points) on a generic aerodrome; sampling time equal to the SMR scan time = 1 s.

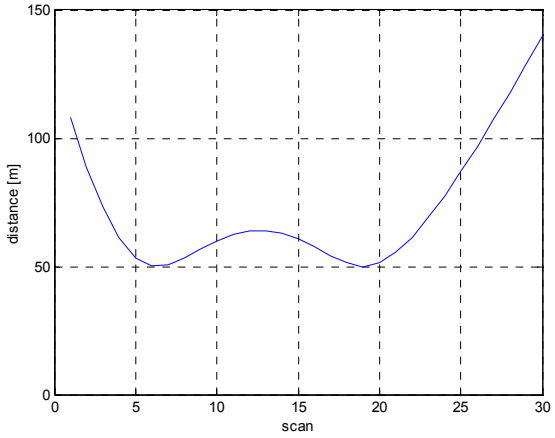

Figure 5. Distance between the aircraft and the car as a function of the radar scan number.

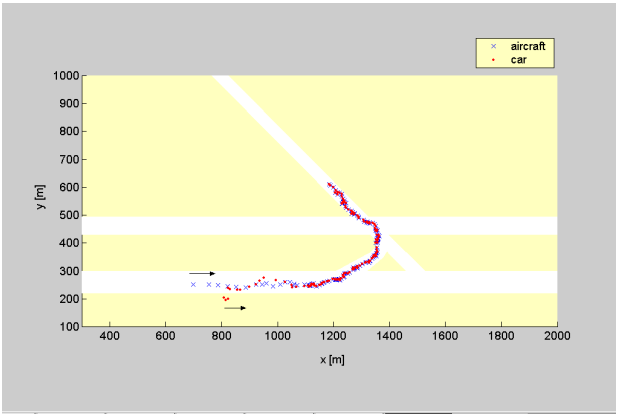

Figure 6. Estimated tracks of the aircraft (blue crosses) and the vehicle (red points); example in which the overlapping of the correlation gates has caused a track collapsing.

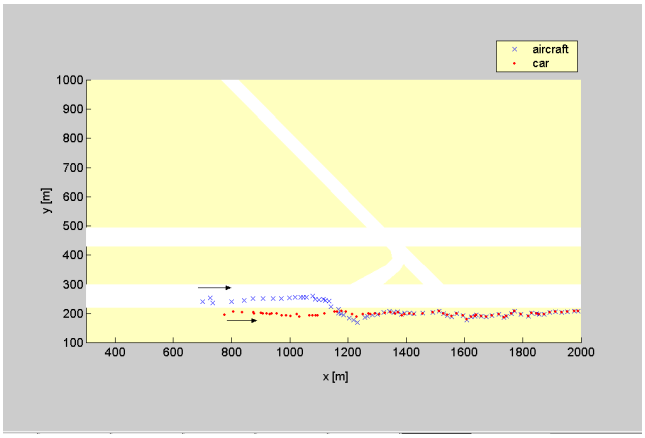

Figure 7. Estimated tracks of the aircraft (blue crosses) and the vehicle (red points); example in which the overlapping of the correlation gates has caused a track collapsing.

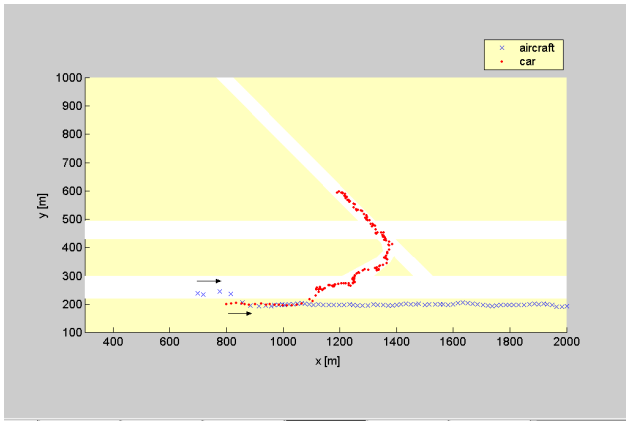

Figure 8. Estimated tracks of the aircraft (blue crosses) and the car (red points); example in which the overlapping of the correlation gates has caused a track swapping.

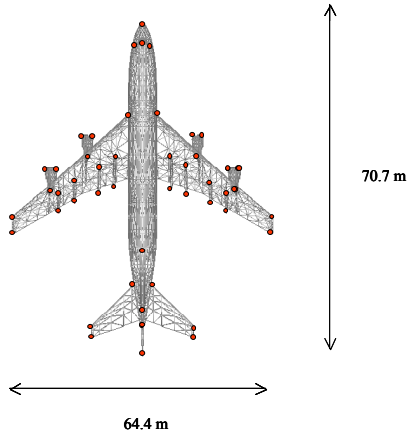

Figure 9. CAD model of a Boeing 747; the hot spots are shown on the model.

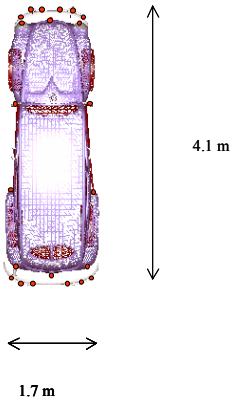

Figure 10. CAD model of a Volkswagen Beetle; the hot spots are shown on the model.

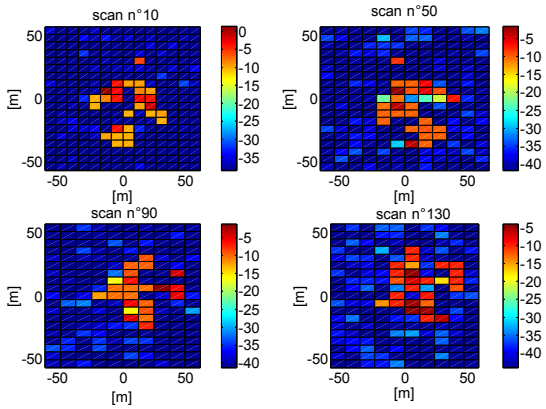

Figure 11. Example of Boeing 747 electromagnetic images along the trajectory of Figure 4 (scans n° 10, 50, 90 and 130).

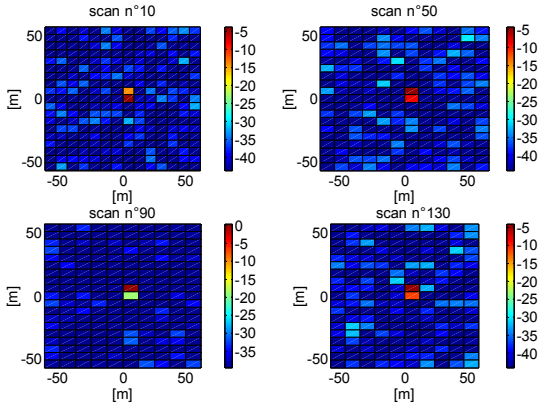

Figure 12. Example of car electromagnetic images along the trajectory of Figure 4 (scans n° 10, 50, 90 and 130).

5 Simulation results without using the electromagnetic images

In this section the results obtained by a simple Nearest Neighbour (NN) plot-to-track association logic [2] which uses just kinematics information are reported. Two different filtering algorithms have been considered: an Extended Kalman Filter (EKF) and a Variable Structure - Interactive Multiple Model (VS-IMM) which uses kinematics constraints to improve the accuracy (for details, see [1]).

Table 1 and Table 2 show the results obtained respectively for the aircraft and the car in terms of number of correct, lost and swapped tracks. The results have been averaged over 1000 Monte Carlo trials.

Consider the EKF algorithm. The overlapping of the correlation gates of the two tracks in the first thirty scans causes frequent tracking errors. The aircraft is correctly tracked in only the 59% of the trials; in the 27.4% of the cases the algorithm loses the tracking, while in the 13.6% of the trials the algorithm, after tracking for some plots the aircraft, erroneously follows the car. The car is correctly tracked in only the 76.1% of the cases; in the 8.1% of the trials the algorithm loses the tracking; while in the 15.8 % of the cases the algorithm, after tracking for some plots the car, erroneously tracks the aircraft. The performance is better for the car because it goes straight while the aircraft is manoeuvring.

Consider the VS-IMM. The use of constraints to the motion of the two targets sensibly improves the tracking performance. The case in which the algorithm loses the aircraft are reduced of the 87%, while the one in which it loses the car are reduced of the 47%. The cases in which the algorithm follows the car, after tracking the aircraft, are reduced of the 12% while the ones in which it follows the aircraft, after tracking the car, are reduced of 64%.

Table 1. Correct, lost and swapped tracks of the aircraft for two tracking algorithms using the NN plot-to-track association logic and kinematics data.

	Correct [%]	Lost [%]	Swapped [%]
EKF	59.0%	27.4%	13.6%
VS-IMM	84.3%	3.6%	12.0%

Table 2. Correct, lost and swapped tracks of the car for two tracking algorithms using the NN plot-to-track association logic and kinematics data.

	Correct [%]	Lost [%]	Swapped [%]
EKF	76.1%	8.1%	15.8%
VS-IMM	90.0%	4.3%	5.7%

6 Simulation results using the electromagnetic images

In this section we report the results obtained by using the target electromagnetic image provided by the SMR in the plot-to-track correlation logic as indicated in the sections 2 and 3. Table 3 and Table 4 show the results obtained respectively for the aircraft and the car in terms of number of correct, lost and swapped tracks. Also in this analysis the results have been averaged over 1000 Monte Carlo trials.

It can be seen that with respect to the case of the plot-to-track correlation algorithm based on the NN association logic and kinematics measurements, the number of lost and swapped tracks is drastically reduced.

Consider the EKF algorithm. By using the electromagnetic images the number of lost tracks is reduced of the 77% in the case of the aircraft and of the 93% in the case of the car. The number of tracks in which the algorithm follows the car, after tracking for some plots the aircraft, is reduced of the 82%; the number of tracks in

which the algorithm follows the aircraft, after tracking the car, is reduced of 100%.

Consider the VS-IMM algorithm. By using the electromagnetic images the number of lost tracks is reduced of the 80% in the case of the aircraft and of the 95% in the case of the car. The number of tracks in which the algorithm follows the car, after tracking for some plots the aircraft, is reduced of the 75%; the number of tracks in which the algorithm follows the aircraft, after tracking the car, is reduced of 100%.

Table 3. Correct, lost and swapped tracks of the aircraft for two tracking algorithms using the plot-to-track association logic described in sections 2 and 3.

	Correct [%]	Lost [%]	Swapped [%]
EKF	91.2%	6.3%	2.5%
VS-IMM	94.9%	2.8%	2.3%

Table 4. Correct, lost and swapped tracks of the car for two tracking algorithms using the plot-to-track association logic described in sections 2 and 3.

	Correct [%]	Lost [%]	Swapped [%]
EKF	99.5%	0.5%	0.0%
VS-IMM	99.8%	0.2%	0.0%

7 Simulation results using the electromagnetic images (scenario with two similar targets)

Here we illustrate the results obtained by considering a second aircraft instead of a car. The scope of this simulation is to test the discrimination capability of the plot-to-track association algorithm in the worst case: two similar target moving in the same direction.

The results concerning the NN plot-to-track logic are reported in Table 5 and Table 6 (aircraft 1 is the manoeuvring one while aircraft 2 is the one going straight). The performance are worse than the ones of the case with the car because the measurement of the second aircraft is noisier due to the greater glint phenomenon. The use of VS-IMM still improves the tracking performance: the cases in which the algorithm loses the manoeuvring aircraft are reduced of the 82%, while the ones in which it loses the aircraft going straight are reduced of the 57%; the cases in which the algorithm follows the aircraft going straight, after tracking the manoeuvring aircraft, are reduced of the 61%, while the ones in which it follows the manoeuvring aircraft, after tracking the aircraft going straight, are reduced of the 52%.

Table 5. Correct, lost and swapped tracks of the aircraft 1 for two tracking algorithms using the NN plot-to-track association logic and kinematics data.

	Correct [%]	Lost [%]	Swapped [%]
EKF	40.0%	33.2%	26.8%
VS-IMM	83.6%	5.9%	10.5%

Table 6 Correct, lost and swapped tracks of the aircraft 2 for two tracking algorithms using the NN plot-to-track association logic and kinematics data.

	Correct [%]	Lost [%]	Swapped [%]
EKF	29.5%	26.8%	43.7%
VS-IMM	67.4%	11.5%	21.1%

The results concerning the plot-to-track association logic using both kinematics data and the electromagnetic images are reported in Table 7 and Table 8.

Consider the EKF algorithm. By using the electromagnetic images the number of lost tracks are reduced of the 78% in the case of the manoeuvring aircraft and of the 51% in the case of the aircraft going straight. The number of tracks in which the algorithm follows the aircraft going straight, after tracking for some plots the manoeuvring aircraft, is reduced of the 71%; the number of tracks in which the algorithm follows the manoeuvring aircraft, after tracking the aircraft going straight, is reduced of 51%.

Consider the VS-IMM algorithm. By using the electromagnetic images the number of lost tracks are reduced of the 54 % in the case of the manoeuvring aircraft and of 16% in the case of the aircraft going straight. The number of tracks in which the algorithm follows the aircraft going straight, after tracking for some plots the manoeuvring aircraft, is reduced of the 84%; the number of tracks in which the algorithm follows the manoeuvring aircraft, after tracking the aircraft going straight, is reduced of 66%.

It can be noted that the results are worse than the ones reported in the previous section, but the improvement obtained by using images is still appreciable. The algorithm is in fact able to discriminate the two targets thanks to the different angles of view (between 2° and 6° degrees in the first thirty scans, see Figure 13) and the performance remains much higher than the one obtained by the simple NN algorithm and kinematics measurements. The different viewing angle in fact gives rise to different electromagnetic images of the two targets.

Table 7. Correct, lost and swapped tracks of the aircraft 1 for two tracking algorithms using the plot-to-track association logic described in sections 2 and 3.

	Correct [%]	Lost [%]	Swapped [%]
EKF	84.9%	7.4%	7.7%
VS-IMM	95.1%	3.2%	1.7%

Table 8. Correct, lost and swapped tracks of the aircraft 2 for two tracking algorithms using the plot-to-track association logic described in sections 2 and 3.

	Correct [%]	Lost [%]	Swapped [%]
EKF	65.6%	13.2%	21.2%
VS-IMM	83.3%	9.6%	7.1%

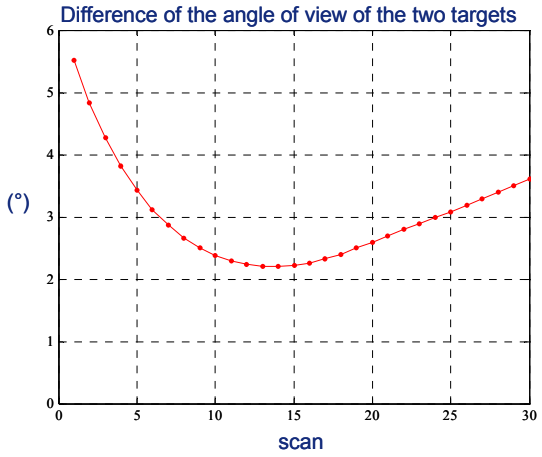

Figure 13. Difference of the angle of view of the two targets relative to the trajectories shown in Figure 4.

8 Conclusions

This paper has shown the great advantage of incorporating the electromagnetic target image in the plot-to-track correlation logic in addition to the classical position measurements. The probabilities of either track swapping or track coalescing are greatly reduced. The next investigation step is to determine which is the effect of multipath in the formation of the electromagnetic image of target and the corresponding impact on performance of the plot-to-track correlation logic. In fact, one of the most severe phenomenon affecting the A-SMGCS performance is the presence of multiple unwanted scattering from the many buildings and infrastructures present in the aerodrome; the multipath phenomenon ultimately set the limit to the tracking system performance. The multipath phenomenon needs to be modeled via an accurate electromagnetic reproduction of the scattering from the aerodrome buildings: a task that requires the three-dimensional modeling of the aerodrome infrastructures and the availability of powerful electromagnetic software tools (e.g.: based on the ray tracing method) to calculate the electromagnetic scattering, thus allowing us to characterize accurately the multipath phenomenon. Another investigation area will be the performance analysis when the detection probability, P_d, of the radar is < 1 and the false alarm probability is > 0. Finally the role of the SMR resolution on the tracking performance should be investigated too.

References

[1] A. Farina, L. Ferranti, G. Golino. Constrained tracking filters for A-SMGCS. *Proc. Sixth Int. Conf. Information Fusion*, Cairns, Queensland, Australia, 8–11 July 2003.

[2] A. Farina, F.A. Studer. *Radar Data Processing. Introduction and Tracking (vol. I)*. Research Studies Press (England), John Wiley & Sons (USA), May 1985.

[3] D. R. Wehner. *High Resolution Radar*. Artech House, 1987.